## 1.1 Molecular imaging techniques for dementia

Molecular imaging aims to quantify brain abnormalities by modeling interactions between a PET radiopharmaceutical and various process of interest such as metabolism, neuroinflammation, or the presence of abnormal proteins in the brain. Despite of limited spatial resolution (~6mm) PET and SPECT associated with specific molecular probes have high sensitive to detect biological process in the order of picomolar ($10^{-12}$). Methodology involved in molecular imaging is summarized in the figure 1. The high sensitivity to quantify focal neuropathological events in the living human brain makes PET the ideal imaging modality for diagnosing and staging neurodegenerative diseases.

## 1.1 New [$^{18}$F] amyloid imaging agents

Although [$^{11}$C]PIB has played an important role as a proof-of-concept for amyloid imaging in dementia (see above), it is not suitable for large-scale studies or clinical use due to the short half life (20 min) of [$^{11}$C] . In contrast, the longer half life (110 min) of [$^{18}$F] allows amyloid imaging agents labeled with this radioisotope to be produced at a central cyclotron sites and delivery to the clinical PET facilities in a large catchment area. [$^{18}$F]florbetapir, [$^{18}$F]florbetaben and [$^{18}$F]flutemetamol are currently undergoing clinical trials to establish their suitability for accurately image amyloid pathology in clinical and preclinical context. Similarly to [$^{11}$C]PIB, these amyloid agents binds to fibrillary amyloid conformations [1] [2] [3]. As a rule, the brain uptake of amyloid radioligands highly depends on patient's age and APOE4 status [4]. The high white matter uptake observed in this first generation of [$^{18}$F]amyloid imaging agents represents a

disadvantage in comparison with [$^{11}$C]PIB. The general properties of these new [$^{18}$F]imaging agents are summarized in the table 1.

[$^{18}$F]florbetapir (also known as Amyvid (TM), or [$^{18}$F]AV45) is a styrylpyridine that can be easily synthetized and distributed [5]. [$^{18}$F]florbetapir is the amyloid agent utilized by ADNI [5] and it has recently obtained USA Food and Drug Administration (FDA) approval as a clinical agent for detecting in vivo brain amyloid neuritic plaques density in dementia patients [6]. Typically, imaging acquisition protocols consist of a 10 minutes acquisition starting from 30-50 min after a 150-300 MBq [$^{18}$F]florbetapir venous bolus injection. Pre-mortem [$^{18}$F]florbetapir images have excellent correlation with post-mortem neuropathology outcomes [7]. [$^{18}$F]florbetapir scans can either be qualitatively interpreted or semi quantified as a brain to cerebellum ratio (BCR). Qualitative interpretation relies on the high white matter and low gray matter [$^{18}$F]florbetapir uptake. A normal [$^{18}$F]florbetapir scan is characterized by high white/gray matter contrast (see figure 2). In contrast, an abnormal scan is characterized by the a focal increase of cortical [$^{18}$F]florbetapir uptake in comparison with the adjacent white matter; or reduction between gray /white matter delineation in at least two brain areas. Negative scans indicates sparse to no neuritic plaques, and is inconsistent with a neuropathological diagnosis of AD at the time of image acquisition. Thus a negative scan indicated reduced the likelihood that a patient's has AD. A positive [$^{18}$F]florbetapir scan indicates moderate to frequent amyloid neuritic plaques. However, neuropathological examination has shown that amyloid neuritic plaques is present not only in patients with AD, but it may also

be present in patients with other types of neurologic conditions as well as older people with normal cognition. Semi quantitative analysis is considered abnormal when BCR is above 1.17, although variations on the [$^{18}$F]florbetapir cut-off values have been proposed [7, 8]. In cognitively normal individuals high [$^{18}$F]florbetapir uptake has been associated with poor processing speed, working memory, and reasoning [4]. Correlations between [$^{18}$F]florbetapir uptake and cognition is absent in MCI or AD patients. Characteristically, AD patients have [$^{18}$F]florbetapir BCR is higher than 1.3, while MCI and controls have 1.2 and 1.0 respectively [9]. Although brain permeable demethylated and an acetylated [$^{18}$F]florbetapir metabolites constitute a drawback for amyloid quantification, permeable radiometabolites do not reduce the reproducibility of [$^{18}$F]florbetapir quantification [2]. In fact, [$^{18}$F]florbetapir has demonstrated optimal reproducibility and high sensitivity to detect amyloid accumulation although in clinical settings, visual analysis of [$^{18}$F]florbetapir has been reported inferior to semi quantitative analysis [10 11].

[$^{18}$F]flutemetamol (also known as [$^{18}$F]GE-067) is a fluoro-derivative of [$^{11}$C]PIB. Typical imaging protocols consist of a 30 minutes acquisition starting 90 min after a 150-300 MBq [$^{18}$F]flutemetamol venous bolus injection. [$^{18}$F]flutemetamol images are suitable for visual or semi-quantitatively analyses using BCR [12]. Comparison between [$^{18}$F]flutemetamol in vivo imaging (BCR) with in vitro biopsied specimens histopathology reveal excellent correlation with in vivo in vitro correlations [7]. [$^{18}$F]flutemetamol has sensitivity of 93% specificity of

93% and high reproducibility (1–4% test-retest variability) [13]. BCR for AD, MCI and controls is 2.2, 1.5 and 1.1, respectively [14] [13].

The stilbene derivative [$^{18}$F]florbetaben (also known as BAY-94-9172, AV-1) can be easily synthesized [15]. The typical imaging acquisition protocol consists of a 20 minutes acquisition starting 90 min after a 300 MBq venous [$^{18}$F]florbetaben bolus injection [16]. [$^{18}$F]florbetaben images can be visually assessed or semi-quantified using BCR. High reproducibility has been achieved with both analytical methods. [16]. BCR for AD and controls are 2.0, 1.6 and 1.2 respectively [17]. [$^{18}$F]florbetaben diagnostic sensitivity has been reported between 100 - 80% and specificity was 91%. [18] [17]. In comparison with [$^{11}$C]PIB, [$^{18}$F]florbetaben has demonstrated good performance, however with a slightly lower dynamic range [19].

A second generation of [$^{18}$F] amyloid imaging agents is current on phase I-II studies. These new compounds bring the promise to broad the short dynamic range of present amyloid agents, which will ultimately translates into a better discrimination between AD, MCI and controls. In comparison with the first generation of [$^{18}$F]amyloid agents, [$^{18}$F]AZD4694 displays faster kinetics, lower white matter binding and no brain-permeable metabolites. [$^{18}$F]AZD4694 is suitable for fully full quantification in 45 min or semiquantification (BCR) obtained for 10 minutes as early as 50 min after a 200–300 MBq venus bolus injection. There is no studies evaluating [$^{18}$F]AZD4694 qualitative readings. [$^{18}$F]AZD4694 measures show good reproducibility [20].

### 1.1 Biomarkers of tissue pathology

Only a small fraction of the 4820 molecular probes listed at the Molecular Imaging Probes & Contrast Agents database (http://www.ncbi.nlm.nih.gov/books/NBK5330/) have been tested in Alzheimer's disease. Together with imaging biomarkers of amyloidosis or neurodegeneration, molecular imaging research in AD has contributed for a better understanding of various aspects underlying AD pathology such presynaptic adaptations, synaptic fluctuations of neurotransmitters, postsynaptic neuroreceptor plasticity and accumulation abnormal proteins in the brain. Although still far from clinical use, imaging agents, here designated as "biomarkers of tissue pathology", have potential applications for monitoring disease progression and evaluating the effects of new pharmacological interventions. In summary, biomarkers for AD tissue pathology are indicators of neuroreceptor systems, neuroinflammation, microglial activation or astrocytosis (table 2).

Regional neuroreceptors declines in AD brain reflect either cell depletion, downregulation or membrane protein conformational changes. So far, although depleted in AD, there is no immediate clinical applications for the use of histamine $H_{1,}$ opiates Mu and adenosine A2 imaging in dementia [21, 22 23].

There very limited clinical application for dopamine receptor PET images in AD although changes in dopamine receptors are associated with neuropsychiatric and cognitive aspects of AD, multiple system atrophy and Huntington's disease. The use of dopamine receptor PET images (i.e [$^{11}$C]raclopride) can be considered in the differential diagnosis of striatal-specific

neurodegeneration (i.e Huntington's disease, multiple system atrophy). Moreover, dopamine $D_{2/3}$ receptor concentrations measured with PET [$^{11}$C]FLB in the hippocampus correlates with cognitive function. Reduced $D_1$ receptors in the cortex and striatum (measured with PET [$^{11}$C]SCH23390) [27] [28] have been also reported in AD.

In contrast, stability of presynaptic dopamine projections have been clinically explored in the differential diagnosis between AD and synucleinopathies. Radiopharmaceuticals for dopamine transporter or monoamine vesicular transporter (DAT, [$^{11}$C]DTBZ) are particularly useful to detect depletion of dopamine projections as seen in LBD or PD [24-26].

It has been proposed a potential clinical application for serotonin 5-$HT_{1A}$ [$^{18}$F]MPPF scans since they are more sensitive than [$^{18}$F]FDG to reveal hippocampal neurodegeneration in AD. However, it remains controversial whether 5-$HT_{1A}$ declines initiates during the MCI phase [29-31]. A role for serotonin 5-$HT_{2A}$ imaging with [$^{18}$F]altanserin has been proposed to for early detection of AD since 5-$HT_{2A}$ receptors are depleted in MCI stage in a level that exceeds serotonin degeneration measured with [$^{11}$C]DASB [32-36]. However, 5-$HT_{2A}$ data needs replication, and analysis of 5-$HT_{2A}$ images is too complex for clinical settings. Interestingly, serotonin 5-$HT_4$ receptor measured with [$^{11}$C]SB207145 remains stable in the brain of AD patients [37].

Although cholinergic hypothesis for AD has a significant impact on AD therapeutics, cholinergic imaging has a modest impact on the diagnosis of AD. Cholinergic nicotinic receptors measured by PET [$^{11}$C]nicotine are reduced in the

cortex of AD.[38, 39] In fact, acetylcholine nicotinic α4β2 receptor availability revealed by 2-[18F]FA-85380 is already reduced in MCI stage [40, 41]. Quantification of brain acetylcholinesterase density has been a complex task to achieve with PET [42, 43]. Although donepezil has a high selectivity for acetylcholinesterase, [$^{11}$C]donepezil PET does not seem to convey the distribution of brain concentrations of acetylcholinesterase [44, 45]. In contrast, PET tracers such as N-methylpiperidine-4-yl propionate ([$^{11}$C]PMP) and N-11C-methylpiperidyl-4-yl acetate ([$^{11}$C]MP4A) are acethylcholinesterase substrates employed to estimate acetylcholinesterase activity [46 47 48]. Correlation between cortical acetylcholinesterase activity and attention measures supports the clinical therapeutic value of anticholinesterase inhibitors [49 50]. PET [$^{11}$C]PMP and [$^{11}$C]MP4A have demonstrated reduced anticholinesterase activity in MCI converters, AD, LBD and PDD compared with healthy controls [51 52 53]. In fact, basal acetylcholinesterase activity predicts therapeutic effects of cholinesterases inhibitors [54].

Neuroinflammation is a neuropathological feature of numerous neurodegenerative conditions. PET allows for in vivo quantification of various aspects of neuroinflammatory responses, which may serve to monitor the effects of pharmacological interventions. High phospholipase enzymatic activity can be detected by the increased unidirectional trapping of [$^{11}$C]arachidonic acid in the AD brain [55, 56].

Astrocytosis can be demonstrated in vivo by the PET [$^{11}$C]deprenyl / dutodeprenyl, which irreversibly binds to the astrocytic enzyme monoamine

oxidase B (MAO-B). [$^{11}$C]d-L-Deprenyl PET scans show increased astrocytic activity in the hippocampus and basal ganglia of AD parients [57, 58]. Study of patients with AD and Creutzfeldt–Jacob disease have shown increase of brain [$^{11}$C]deprenyl binding [57-59].

PET also reveal microglial activation detected via the overexpression of the peripheral benzodiazepine receptor/translocator protein (TSPO) system with [$^{11}$C]PK1195, [$^{11}$C]DAA1106 and [$^{11}$C]vinpocetine [59]. Increased of microglial activation observed by the TSPO binding have been shown in AD, FTD, LBD, CBS, PSP and other neurodegenerative conditions [60 61-64].

Finally, an important advance on molecular imaging of dementia is the introduction of molecular probes specific for neurofibrillary tangles. The radioligand [$^{18}$F]THK523 is a candidate for imaging neurofibrillary tangles in late phase of preclinical characterization. [$^{18}$F]THK523 has high affinity for tau preparations and a low affinity for synthetic Aβ1-42 fibrils and consequently binds to neurofibrillary tangles in human brain tissue without appreciable labeling of diffuse Aβ plaques. Radiopharmaceuticals able to quantify tau pathology in the human brain are highly needed to advance the diagnosis and possible guide therapeutic interventions in neurodegenerative diseases.

In conclusion, although Canada has a good imaging infrastructure and most of these radioligands are available for human use, it seems premature the widespread use of imaging tools to diagnose AD. Particularly regarding the use of [$^{18}$F]florbetapir, it seems reasonable to have its use restricted to specific clinical circumstances or clinical trials (see above recommendations for PIB).

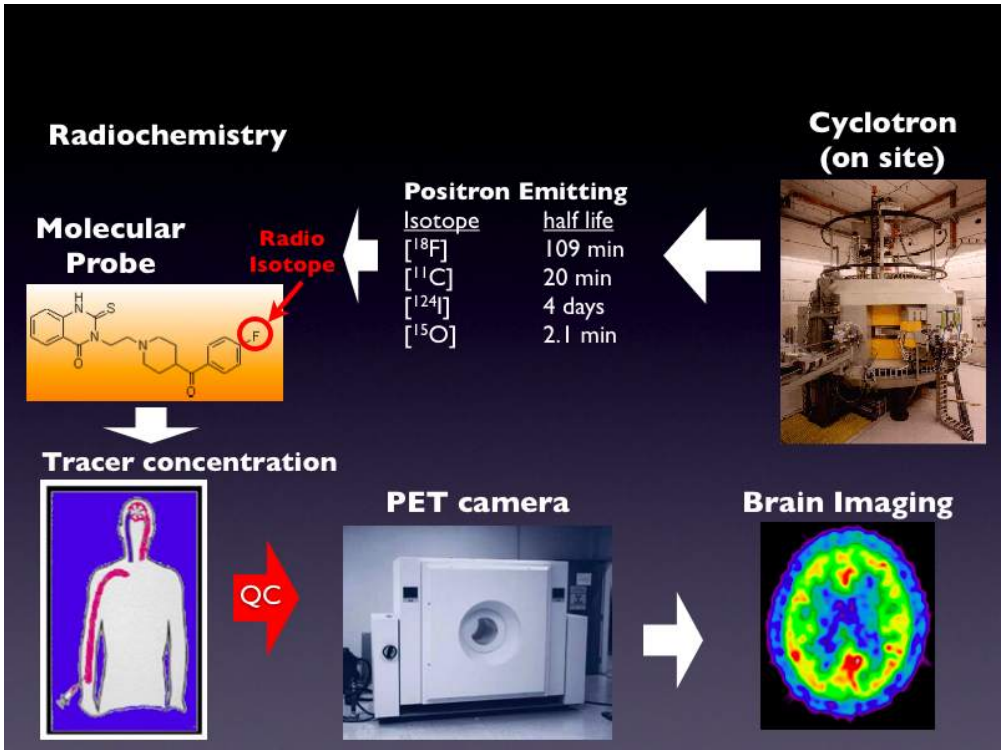


**Figure 1. Overview of the procedures involved in a PET scan.** Production of radioisotopes for a PET scans requires short-lived positron-emitting radioisotopes. The cyclotron produces the radiophamaceuticals and and the radiopharmacy synthesises, conduct quality control, packs and delivers PET-molecular probes to hospitals and research centres. PET scan requires the venous injection of a infinitesimally low dose if the molecular probe. The PET camera records the dynamic distribution of radioactivity during the time-course of a study. In general, images of the brain concentration of radiopharmaceuticals are utilized for clinical reading.

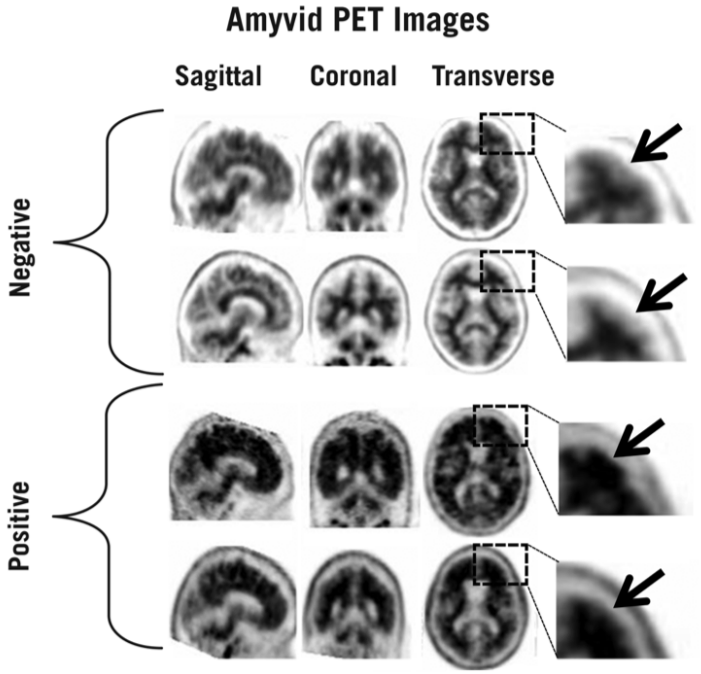


Figure 2: Examples of Amyvid negative scans (top two rows) and positive scans (bottom two rows). Left to right panels show saggital, coronal and transverse PET images slices. Final panel shows enlarged picture of the brain area under the box. The top two arrows are pointing to normal preserved gray-white contrast with the cortical radioactivity less than the adjacent white matter. The bottom two arrows indicate areas of decreased gray-white contrast with increased cortical radioactivity that is comparable to the radioactivity in the adjacent white matter (extracted from Amyvid prescribing information – Eli lilly and Company).

Table 1. Summary of new [18F] amyloid agents

| Biological Process of interest | Phase | Chemical group | Plasma metabolite | Scan duration |
|---|---|---|---|---|
| **Differential Diagnosis** | | | | |
| [$^{18}$F]florbetapir (AV45) | III | Styrylpyridine | Polar and apolar | 10 min |
| [$^{18}$F]florbetaben (BAY94-9172) | III | Stilbene | Polar and apolar | 10-20 min |
| [$^{18}$F]flutemetamol | III | Benzothiazole | Polar | 10-20 min |
| [$^{18}$F][$^{18}$F]AZD4694 | II | Benzothiazole | Polar | 10-20 min |

Table 2. Summary of Biomarkers of tissue pathology

| Biological Process of interest | Radioligand | Changes on the binding parameters expected in in AD | Interpretation | Possible application |
|---|---|---|---|---|
| **Differential Diagnosis** | | | | |
| Tau pathology | [$^{18}$F]THK523 | Increases | Increased neurofibrillary tangless | Presence of tau pathology |
| Monoamine vesicular transporter | [$^{11}$C]DTBZ | Declines | Nigro- striatal or mesolimbic Neurodegeneration | Diagnosis or comorbidity with LBD |
| **Pathological features** | | | | |
| **Inflammation** | [$^{11}$C]PK11195 | Increas | Microglial activation | Disease modifying |

| | | | | |
|---|---|---|---|---|
| | | es | | therapy |
| **Pre-synaptic neurodegeneration** | | | | |
| **Acethylcholine vesicular transporter** | [$^{18}$F]FEOBV<br>[$^{123}$I]IBVM | Declines | Cholinergic forebrain neurodegeneration | Early diagnosis |
| **Post-synaptic neurodegeneration** | | | | |
| **Serotonin 5-HT2A** | [$^{18}$F]altanserin | Declines | Cortical neurodegeneration | Early diagnosis<br>or<br>Monioring interventions |
| **Serotonin 5-HT1A** | [$^{18}$F]MPPF | Declines | Hippoamppal neurodegenetation | |
| **Dopamine D1 receptors** | [$^{11}$C]SCH1 | Declines | Cortical neurodegeneration | |
| **Dopamine D2 receptors** | [$^{11}$C]raclopride<br>[$^{18}$F]fallypride<br>[$^{11}$C]FLB | Declines | Striatal neurodegeneration<br>Hippocampal neurodegeneration<br>Hippocampal neurodegeneration | |
| **Muscarinic cholinergic receptors** | [$^{11}$C]NMPB | Declines | Cortical Neurodegeneration | |
| **Nicotinic cholinergic receptors** | [$^{18}$F]FP-TZTP | Declines | Cortical Neurodegeneration | |
| **Enzymatic activity** | | | | |
| **acetylcholinesterase** | [$^{11}$C]PMP<br>[$^{11}$C]MP4A<br>[$^{11}$C]MP4B | Declines | Activity of brain cholinesterase | Estimate efficacy of anticholinesterase inhibitors |
| **Phospholipase** | [$^{11}$C]Aracnoid acid | increses | Phospholipase activity | Neuroinflammation |
| **Brain acetylcholinesterase** | | | | |
| | [$^{11}$C]physostigmine<br>[$^{11}$C]tacrine<br>[$^{11}$C]donepezil | Declines | Acethylcholinesterase inhibitors biodistribution | Therapeutic studies |
| | | | | |
| | | | | |

1. Ikonomovic MD, Klunk WE, Abrahamson EE, et al. Post-mortem correlates of in vivo PiB-PET amyloid imaging in a typical case of Alzheimer's disease. Brain 2008;131:1630-1645.
2. Choi SR, Golding G, Zhuang Z, et al. Preclinical Properties of 18F-AV-45: A PET Agent for A Plaques in the Brain. Journal of Nuclear Medicine 2009;50:1887-1894.
3. Wolk DA, Grachev ID, Buckley C, et al. Association Between In Vivo Fluorine 18-Labeled Flutemetamol Amyloid Positron Emission Tomography Imaging and In Vivo Cerebral Cortical Histopathology. Archives Of Neurology 2011.
4. Rodrigue KM, Kennedy KM, Devous MD, et al. β-Amyloid burden in healthy aging: Regional distribution and cognitive consequences. Neurology 2012;78:387-395.
5. Liu Y, Zhu L, Plössl K, et al. Optimization of automated radiosynthesis of [18F]AV-45: a new PET imaging agent for Alzheimer's disease. Nuclear Medicine And Biology 2010;37:917-925.
6. Anon. Conditional Nod to Florbetapir. Journal of Nuclear Medicine 2011;52:26N-26N.
7. Clark CM, Schneider JA, Bedell BJ, et al. Use of florbetapir-PET for imaging beta-amyloid pathology. JAMA: The Journal of the American Medical Association 2011;305:275-283.
8. Fleisher AS, Chen K, Liu X, et al. Using Positron Emission Tomography and Florbetapir F 18 to Image Cortical Amyloid in Patients With Mild Cognitive Impairment or Dementia Due to Alzheimer Disease. Archives Of Neurology 2011.
9. Wong DF, Rosenberg PB, Zhou Y, et al. In vivo imaging of amyloid deposition in Alzheimer disease using the radioligand 18F-AV-45 (florbetapir [corrected] F 18). Journal of nuclear medicine : official publication, Society of Nuclear Medicine 2010;51:913-920.
10. Joshi AD, Pontecorvo MJ, Clark CM, et al. Performance Characteristics of Amyloid PET with Florbetapir F 18 in Patients with Alzheimer's Disease and Cognitively Normal Subjects. Journal of nuclear medicine : official publication, Society of Nuclear Medicine 2012.
11. Camus V, Payoux P, Barré L, et al. Using PET with (18)F-AV-45 (florbetapir) to quantify brain amyloid load in a clinical environment. European Journal of Nuclear Medicine and Molecular Imaging 2012.
12. Nelissen N, van Laere K, Thurfjell L, et al. Phase 1 study of the Pittsburgh compound B derivative 18F-flutemetamol in healthy volunteers and patients with probable Alzheimer disease. Journal of Nuclear Medicine 2009;50:1251-1259.
13. Vandenberghe R, van Laere K, Ivanoiu A, et al. 18F-flutemetamol amyloid imaging in Alzheimer disease and mild cognitive impairment: a phase 2 trial. Annals Of Neurology 2010;68:319-329.
14. Thomas BA, Erlandsson K, Modat M, et al. The importance of appropriate partial volume correction for PET quantification in Alzheimer's disease. European Journal of Nuclear Medicine and Molecular Imaging 2011;38:1104-1119.
15. Wang H, Shi H, Yu H, Jiang S, Tang G. Facile and rapid one-step radiosynthesis of [(18)F]BAY94-9172 with a new precursor. Nuclear Medicine And Biology 2011;38:121-127.
16. Patt M, Schildan A, Barthel H, et al. Metabolite analysis of [18F]Florbetaben (BAY 94-9172) in human subjects: a substudy within a proof of mechanism clinical trial. Journal of Radioanalytical and Nuclear Chemistry 2010;284:557-562.

17. Rowe CC, Ackerman U, Browne W, et al. Imaging of amyloid beta in Alzheimer's disease with 18F-BAY94-9172, a novel PET tracer: proof of mechanism. The Lancet Neurology 2008;7:129-135.
18. Barthel H, Gertz H-J, Dresel S, et al. Cerebral amyloid-β PET with florbetaben (18F) in patients with Alzheimer's disease and healthy controls: a multicentre phase 2 diagnostic study. Lancet Neurology 2011;10:424-435.
19. Villemagne VL, Mulligan RS, Pejoska S, et al. Comparison of 11C-PiB and 18F-florbetaben for Aβ imaging in ageing and Alzheimer's disease. European Journal of Nuclear Medicine and Molecular Imaging 2012.
20. Cselenyi Z, Jonhagen ME, Forsberg A, et al. Clinical Validation of 18F-AZD4694, an Amyloid- -Specific PET Radioligand. Journal of Nuclear Medicine 2012;53:415-424.
21. Higuchi M, Yanai K, Okamura N, et al. Histamine H(1) receptors in patients with Alzheimer's disease assessed by positron emission tomography. Neuroscience 2000;99:721-729.
22. Cohen R, Andreason P, Doudet D, Carson R, Sunderland T. Opiate receptor avidity and cerebral blood flow in Alzheimer's disease. Journal of the neurological sciences 1997;148:171-180.
23. Fukumitsu N, Ishii K, Kimura Y, et al. Adenosine A(1) receptors using 8-dicyclopropylmethyl-1-[C-11]methyl-3-propylxanthine PET in Alzheimer's disease. Annals of Nuclear Medicine 2008;22:841-847.
24. Koeppe RA, Gilman S, Junck L, Wernette K, Frey KA. Differentiating Alzheimer's disease from dementia with Lewy bodies and Parkinson's disease with (+)-[11C]dihydrotetrabenazine positron emission tomography. Alzheimer's & dementia : the journal of the Alzheimer's Association 2008;4:S67-76.
25. Gilman S, Koeppe RA, Little R, et al. Striatal monoamine terminals in Lewy body dementia and Alzheimer's disease. Ann Neurol 2004;55:774-780.
26. Koeppe RA, Gilman S, Joshi A, et al. 11C-DTBZ and 18F-FDG PET measures in differentiating dementias. Journal of Nuclear Medicine 2005;46:936-944.
27. Cortés R, Probst A, Palacios JM. Decreased densities of dopamine D1 receptors in the putamen and hippocampus in senile dementia of the Alzheimer type. Brain Research 1988;475:164-167.
28. Kemppainen N, Ruottinen H, Någren K, Rinne JO. PET shows that striatal dopamine D1 and D2 receptors are differentially affected in AD. Neurology 2000;55:205-209.
29. Truchot L, Costes N, Zimmer L, et al. A distinct [18F]MPPF PET profile in amnestic mild cognitive impairment compared to mild Alzheimer's disease. NeuroImage 2008;40:1251-1256.
30. Kepe V, Barrio J, HUANG S, et al. Serotonin 1A receptors in the living brain of Alzheimer's disease patients. Proceedings of the National Academy of Sciences of the United States of America 2006;103:702-707.
31. Truchot L, Costes SN, Zimmer L, et al. Up-regulation of hippocampal serotonin metabolism in mild cognitive impairment. Neurology 2007;69:1012-1017.
32. Marner L, Frokjaer VG, Kalbitzer J, et al. Loss of serotonin 2A receptors exceeds loss of serotonergic projections in early Alzheimer's disease: a combined [C-11]DASB and [F-18]altanserin-PET study. Neurobiology of aging 2012;33:479-487.

33. Meltzer CC, Price JC, Mathis CA, et al. PET imaging of serotonin type 2A receptors in late-life neuropsychiatric disorders. The American journal of psychiatry 1999;156:1871-1878.
34. Hasselbalch SG, Madsen K, Svarer C, et al. Reduced 5-HT2A receptor binding in patients with mild cognitive impairment. Neurobiol Aging 2008;29:1830-1838.
35. Santhosh L, Estok KM, Vogel RS, et al. Regional distribution and behavioral correlates of 5-HT(2A) receptors in Alzheimer's disease with [(18)F]deuteroaltanserin and PET. Psychiatry research 2009;173:212-217.
36. SADZOT B, LEMAIRE C, Maquet P, et al. Serotonin 5ht(2) Receptor Imaging in the Human Brain Using Positron Emission Tomography and a New Radioligand, [F-18] Altanserin - Results in Young Normal Controls. Journal Of Cerebral Blood Flow And Metabolism 1995;15:787-797.
37. Madsen K, Neumann W-J, Holst K, et al. Cerebral Serotonin 4 Receptors and Amyloid-beta in Early Alzheimer's Disease. Journal of Alzheimer's disease : JAD 2011;26:457-466.
38. Kadir A, Almkvist O, Wall A, Långström B, Nordberg A. PET imaging of cortical C-11-nicotine binding correlates with the cognitive function of attention in Alzheimer's disease. Psychopharmacology 2006;188:509-520.
39. Nordberg A, Lundqvist H, Hartvig P, Lilja A, Langstrom B. Kinetic-Analysis of Regional (S)(-)C-11-Nicotine Binding in Normal and Alzheimer Brains - in-Vivo Assessment Using Positron Emission Tomography. Alzheimer Disease & Associated Disorders 1995;9:21-27.
40. Kendziorra K, Wolf H, Meyer PM, et al. Decreased cerebral α4β2* nicotinic acetylcholine receptor availability in patients with mild cognitive impairment and Alzheimer's disease assessed with positron emission tomography. European Journal of Nuclear Medicine and Molecular Imaging 2011;38:515-525.
41. Mitsis E, Reech K, Bois F, et al. 123I-5-IA-85380 SPECT Imaging of Nicotinic Receptors in Alzheimer Disease and Mild Cognitive Impairment. Journal of Nuclear Medicine 2009.
42. BONNOTLOURS S, Crouzel C, PRENANT C, HINNEN F. C-11 Labeling of an Inhibitor of Acetylcholinesterase - [C-11] Physostigmine. Journal of Labelled Compounds and Radiopharmaceuticals 1993;33:277-284.
43. Blomqvist G, Tavitian B, Pappata S, et al. Quantitative measurement of cerebral acetylcholinesterase using. Journal of cerebral blood flow and metabolism : official journal of the International Society of Cerebral Blood Flow and Metabolism 2001;21:114-131.
44. De Vos F, Santens P, Vermeirsch H, et al. Pharmacological evaluation of [11C]donepezil as a tracer for visualization of acetylcholinesterase by PET. Nuclear Medicine And Biology 2000;27:745-747.
45. Snape MF, Misra A, Murray TK, et al. A comparative study in rats of the in vitro and in vivo pharmacology of the acetylcholinesterase inhibitors tacrine, donepezil and NXX-066. Neuropharmacology 1999;38:181-193.
46. Eggers C, Herholz K, Kalbe E, Heiss W-D. Cortical acetylcholine esterase activity and ApoE4-genotype in Alzheimer disease. Neuroscience Letters 2006;408:46-50.

47. Namba H, Irie T, Fukushi K, Iyo M. In-Vivo Measurement of Acetylcholinesterase Activity in the Brain with a Radioactive Acetylcholine Analog. Brain Research 1994;667:278-282.
48. Kilbourn M, Snyder S, Sherman P, Kuhl D. In vivo studies of acetylcholinesterase activity using a labeled substrate, N-[C-11]methylpiperdin-4-yl propionate ([C-11]PMP). Synapse 1996;22:123-131.
49. Bohnen NI, Kaufer DI, Hendrickson R, et al. Degree of inhibition of cortical acetylcholinesterase activity and cognitive effects by donepezil treatment in Alzheimer's disease. Journal Of Neurology Neurosurgery And Psychiatry 2005;76:315-319.
50. Bohnen N, Kaufer D, Hendrickson R, et al. Cognitive correlates of alterations in acetylcholinesterase in Alzheimer's disease. Neuroscience Letters 2005;380:127-132.
51. Rinne J, Kaasinen V, Jarvenpaa T, et al. Brain acetylcholinesterase activity impairment and early Alzheimer's in mild cognitive disease. Journal Of Neurology Neurosurgery And Psychiatry 2003;74:113-115.
52. Bohnen N, Kaufer D, Hendrickson R, et al. Cognitive correlates of cortical cholinergic denervation in Parkinson's disease and parkinsonian dementia. Journal Of Neurology 2006;253:242-247.
53. Shimada H, Hirano S, Shinotoh H, et al. Mapping of brain acetylcholinesterase alterations in Lewy body disease by PET. Neurology 2009;73:273-278.
54. Kasuya M, Meguro K, Okamura N, et al. Greater Responsiveness to Donepezil in Alzheimer Patients With Higher Levels of Acetylcholinesterase Based on Attention Task Scores and a Donepezil PET Study. Alzheimer Disease & Associated Disorders 2011.
55. Esposito G, Giovacchini G, Liow J-S, et al. Imaging Neuroinflammation in Alzheimer's Disease with Radiolabeled Arachidonic Acid and PET. Journal of Nuclear Medicine 2008;49:1414-1421.
56. Duncan RE, Bazinet RP. Brain arachidonic acid uptake and turnover: implications for signaling and bipolar disorder. Current Opinion in Clinical Nutrition and Metabolic Care 2010;13:130-138.
57. Carter SF, Scholl M, Almkvist O, et al. Evidence for Astrocytosis in Prodromal Alzheimer Disease Provided by 11C-Deuterium-L-Deprenyl: A Multitracer PET Paradigm Combining 11C-Pittsburgh Compound B and 18F-FDG. Journal of Nuclear Medicine 2012;53:37-46.
58. Santillo AF, Gambini JP, Lannfelt L, et al. In vivo imaging of astrocytosis in Alzheimer’s disease: an 11C-L-deuteriodeprenyl and PIB PET study. European Journal of Nuclear Medicine and Molecular Imaging 2011.
59. Gulyás B, Vas Á, Tóth M, et al. Age and disease related changes in the translocator protein (TSPO) system in the human brain: Positron emission tomography measurements with [11C]vinpocetine. NeuroImage 2011:1-11.
60. Cagnin A, Rossor M, Sampson E, MacKinnon T, Banati R. In vivo detection of microglial activation in frontotemporal dementia. Annals Of Neurology 2004;56:894-897.
61. Henkel K, Karitzky J, Schmid M, et al. Imaging of activated microglia with PET and [C-11]PK 11195 in corticobasal degeneration. Movement Disorders 2004;19:817-821.

62. Gerhard A, Watts J, Trender-Gerhard I, et al. In vivo imaging of microglial activation with [C-11](R)-PK 11195 PET in corticobasal degeneration. Movement Disorders 2004;19:1221-1226.
63. Gerhard A, Trender-Gerhard I, Turkheimer F, Quinn N, Bhatia K, Brooks D. In vivo imaging of microglial activation with [C-11](R)-PK11195 PET in progressive supranuclear palsy. Movement Disorders 2006;21:89-93.
64. Turner M, Gerhard A, Al-Chalabi A, et al. Mills' and other isolated upper motor neurone syndromes: in vivo study with C-11-(R)-PK11195 PET. Journal Of Neurology Neurosurgery And Psychiatry 2005;76:871-874.